THE ASTROPHYSICAL JOURNAL, 376:505–513, 1991 August 1

VERY SMALL GRAINS AND THE INFRARED COLORS OF GALAXIES

G. HELOU[1]
Infrared Processing and Analysis Center, Jet Propulsion Laboratory, California Institute of Technology
C. RYTER[2]
Service d'Astrophysique, Centre d'Etudes Nucléaires de Saclay, France
AND
B. T. SOIFER[3]
Infrared Processing and Analysis Center, and Division of Physics, Mathematics and Astronomy, California Institute of Technology
Received 1990 May 9; accepted 1991 January 29

ABSTRACT

We use *IRAS* data to study the contribution of very small grains with fluctuating temperature to the infrared emission of disk galaxies and to estimate the variation among galaxies of the abundance of these small grains relative to the larger "classical," thermally stable grains. We argue that the 12 μm emission from spiral galaxies originates in their interstellar medium and compare the integrated *IRAS* colors of galaxies to the *IRAS* colors of local emission within Galactic nebulae. $\Gamma = \nu f_\nu(12\ \mu\text{m})/F(40\text{–}120\ \mu\text{m})$ is advanced as an estimator of the small-to-large grain ratio, and the interpretation of its statistical behavior in samples of galaxies is discussed. In a color-color diagram of the emission from Galactic nebulae, Γ depends only on $\Theta = f_\nu(60\ \mu\text{m})/f_\nu(100\ \mu\text{m})$, decreasing slowly as Θ increases. The same trend is observed for the integrated colors of galaxies and is seen in three different samples: optically selected "normal" spirals in the Virgo cluster, infrared-luminous galaxies from the *IRAS* bright galaxy sample and "cold" galaxies selected for their low ratios of $f_\nu(60\ \mu\text{m})$ to $f_\nu(100\ \mu\text{m})$. The dispersion on Γ is small (rms $\simeq 40\%$) for $\Theta < \frac{1}{3}$, and increases to about a factor of 2 at $\Theta \simeq 1$. We argue that the low dispersion in the "cold" galaxies represents the true dispersion in the small-to-large grain abundance ratio among galaxies, while the larger dispersion among warmer galaxies is a result of increasing effects of optical depth heating of dust by active galactic nuclei, and destruction of small dust grains at high radiative energy densities. The small-to-large grain ratio is found to be roughly constant among normal galaxies with similar metallicities, with a rms dispersion of 40% or less.

Subject headings: galaxies: interstellar matter — galaxies: photometry — interstellar: grains

1. INTRODUCTION

Observations from rockets (Price 1981) and from the *Infrared Astronomical Satellite* (*IRAS*) have shown that the infrared emission of the interstellar medium exhibits an excess in the 5–20 μm range when compared to the radiation expected from "classical" dust grains in thermal equilibrium in the interstellar radiation field (see, for instance, Cox & Mezger 1989; Boulanger & Pérault 1988). Such a classical grain model, made of a mixture of silicate and graphite particles with sizes between 0.005 and 0.25 μm in diameter (e.g., Mathis, Rumpl, & Nordsieck 1977, hereafter MRN; Draine & Lee 1984) provides a good fit to the interstellar extinction and scattering curves from the red to the far-ultraviolet but fails to produce the observed emission spectrum at wavelengths $2\ \mu\text{m} < \lambda < 40\ \mu$m. The infrared excess requires emission at a few hundred kelvins, as demonstrated by Pajot et al. (1986) and cannot be accounted for by the MRN grain model, even when one includes the dust in shells and envelopes around late-type stars (see, for instance Cox, Krugel, & Mezger 1986). Furthermore, the strong excess at 12 and 25 μm is observed in isolated interstellar clouds and diffuse cirrus (Weiland et al. 1986) far from heating sources. Very small grains transiently heated through the absorption of single UV photons were proposed by Andriesse (1978) to explain this infrared excess in the case of M17 and by Sellgren (1984) to interpret measurements in reflection nebulae. The *IRAS* data provided further evidence in support of the very small grain hypothesis. The importance of this new population of interstellar dust is pointed out by the fact that it accounts for about 40% of the infrared emission from the interstellar medium in the solar neighborhood (Boulanger & Pérault 1988; Puget & Léger 1989).

A general, well-defined relationship between the infrared color ratios $f_\nu(12\ \mu\text{m})/f_\nu(25\ \mu\text{m})$ and $f_\nu(60\ \mu\text{m})/f_\nu(100\ \mu\text{m})$ in galaxies was demonstrated by Helou (1986) and related to the contribution of very small grains to the infrared emission. The same behavior of the color ratios was also noted by Pajot et al. (1986). Similar evidence for small grains was found by Ghosh, Drapatz, & Peppel (1986), who compared galactic H II regions to external galaxies, and by Walterbos & Schwering (1987), who showed the infrared colors of M31 to be very similar to those of cirrus in the Milky Way. This paper studies the contribution of very small grains to the infrared emission from galaxies based on our understanding of the corresponding situation in the Milky Way and attempts to estimate the variation among galaxies of the relative abundance of very small to classical grains. The interpretation of the 12 μm emission from the local interstellar medium is reviewed in § 2 and then extended to disk galaxies. The extragalactic samples used in

[1] IPAC 100-22, California Institute of Technology, Pasadena, CA 91125.
[2] Laboratoire de Radioastronomie Millimétrique, Ecole Normale Supérieure, 24 Rue Lhomond, 75005 Paris, France.
[3] Downs lab 320-47, California Institute of Technology, Pasadena, CA 91125.

the study are described in § 3, and a comparison between the Milky Way and external galaxies appears in § 4; the results are presented and discussed in §§ 5 and 6.

2. 12 MICRON EMISSION IN THE LOCAL INTERSTELLAR MEDIUM

Detailed studies of M31 by Walterbos & Schwering (1987), of the Large Magellanic Cloud by Schwering (1988), and of M33 by Rice et al. (1990) demonstrate that the 12 μm emission from these galaxies is associated with their interstellar medium, rather than any component of the stellar population. We therefore assume that this association holds for typical disk galaxies (i.e., those with a substantial interstellar medium) since it holds in the two extreme cases of a quiescent early-type spiral and a late-type irregular.

Classical models of the interstellar dust (e.g., Draine & Lee 1984) fail to reproduce the observed 12 μm emission, thus leading to the suggestion of very small grains radiating in non-equilibrium (Andriesse 1978; Sellgren 1984). On the other hand, several prominent, so-called "unidentified," interstellar spectral features at wavelengths ranging from $\lambda = 3.3$ μm to at least $\lambda = 11.3$ μm (Gillett, Forrest & Merrill 1973; Merrill, Soifer, & Russell 1975; Willner et al. 1977; Russell, Soifer, & Willner 1977; Sellgren, Werner, & Dinerstein 1983; Cohen et al. 1986) have been attributed by Léger & Puget (1984), and by Allamandola, Tielens, & Barker (1985) to polycyclic aromatic hydrocarbons (PAHs) excited by ultraviolet photons. Although debate continues (see, for instance, Allamandola 1989 and Duley 1989), it is already clear that the very small grains and the emitters of the unidentified features either occur in essentially constant ratio to each other, or are the same grains, especially since the emission in the 3.3 μm aromatic feature follows closely the large-scale Galactic structure traced out by the *IRAS* 12 μm band emission (Giard et al. 1989). See Puget & Léger (1989) for a comprehensive review.

Another open question is what fraction of the emission within the *IRAS* 12 μm band is carried by the aromatic features as opposed to the continuum. While Giard et al. (1989) estimate that fraction to be about 40% for the Milky Way as a whole, Ryter, Puget, & Pérault (1987) find that fraction to be essentially one in the reflection nebula NGC 2023 (excited by the B9 star HD 37093), which is practically neutral, and probably a representative piece of the interstellar medium. Spectra of nuclear starbursts in galaxies (especially M82 and NGC 253) show the same suite of spectral features (Gillett et al. 1975; Phillips, Aitken, & Roche 1984) clearly dominating the 12 μm band emission. Similar spectra are also observed with the larger aperture (15″ by 2′) of the *IRAS* Low-Resolution Spectrometer data (*IRAS* Science Team 1986) for M82, NGC 253, and H II regions in the Milky Way. However, because of their unknown zero level, these data cannot be used to address the question of the relative strength of features and continuum.

We therefore adopt the interpretation that the *IRAS* 12 μm band emission from quiescent spiral galaxies originates primarily from very small grains (smaller than 100 Å in radius, consisting mostly of H and C atoms) with fluctuating temperatures, regardless of what fraction of that emission appears as spectral features or as continuum.

3. THE SAMPLES

For the purposes of comparison between the *IRAS* colors of Galactic and extragalactic dust emission, the Galactic data are taken from published studies of three nebulae heated by early-type stars (Ryter, Puget, Pérault 1987; & Boulanger et al. 1988), and from studies of nearby quiescent molecular clouds (Boulanger et al. 1990) which address a different range of heating conditions and reveal quite distinct behavior (see Fig. 1 and § 6 for more details). The extragalactic material consists of three samples of galaxies detailed below. For each object in these samples, the *IRAS* survey data were combined before flux estimation, resulting in substantially improved sensitivity compared to the *IRAS* Point Source Catalog (1988).

3.1. *Galaxies in the Virgo Cluster*

A set of 196 optically selected galaxies located in ~ 250 deg^2 centered on the Virgo cluster has been studied by Helou et al. (1988). Of these, 131 are large "normal" disk galaxies, mostly with morphological type Sa or later. The 65 remaining objects are blue compact dwarfs (BCD) from the catalog by Binggeli, Sandage, & Tammann (1985), none of which were detected at 12 μm (see Helou et al. 1988 for details). Of the spirals (Sa or later), 69 have been detected at 12, 60, and 100 μm and constitute what will be called the Virgo sample in this paper. For an assumed distance to Virgo of 14 Mpc and a corresponding $H_0 = 75$ km s^{-1} Mpc^{-1}, their far-infrared luminosities range from 10^8 to 5×10^9 $L_\odot$.

3.2. *Infrared Bright Galaxies*

Soifer et al. (1987, 1989) have defined a sample containing all 313 extragalactic objects with $f_\nu(60\ \mu\text{m}) > 5.24$ Jy within a 14,500 deg^2 area of the sky (the *IRAS* Bright Galaxy Sample). All 313 objects are galaxies, ranging in distance from the Local Group to 320 Mpc, and in infrared luminosity from 2×10^8 to $\sim 2 \times 10^{12}$ $L_\odot$. The median distance and infrared luminosity in the sample are, respectively, ~ 30 Mpc and $\sim 3.6 \times 10^{10}$ $L_\odot$. This bright galaxy sample is biased toward higher infrared luminosities, in contrast to the Virgo sample, which is basically a volume-limited selection of objects. The two samples do, however, overlap, with 19 objects in common.

3.3. *Cold-Dust Galaxies*

This sample is selected for low color temperatures between 60 and 100 μm, so that the emission from these galaxies is dominated by the cirrus component (Helou 1986). To construct the sample, we started with the *IRAS* Faint Source Catalog version 1.0 (this is the result of a co-addition of the sky at $|b| > 50$; Moshir et al. 1989), which we searched for sources associated with galaxies, with $f_\nu(60\ \mu\text{m}) > 0.5$ Jy, and with $f_\nu(60\ \mu\text{m})/f_\nu(100\ \mu\text{m}) < 0.25$. The search yielded 85 sources, for each of which the *IRAS* data were then co-added using ADDSCAN/SCANPI software (Helou et al. 1988). It turned out many of these sources corresponded to nearby galaxies, unresolved by the *IRAS* detectors at 100 μm, but resolved at 60 μm, leading to underestimation of the 60 μm flux in the Faint Source Catalog. Using the fluxes derived from ADDSCAN/SCANPI, only 46 sources satisfied the slightly relaxed condition $f_\nu 160\ \mu\text{m})/f_\nu(100\ \mu\text{m}) < 0.27$, and only 43 of the 46 were detected at 12 μm.

4. COMPARISON OF *IRAS* COLORS OF GALACTIC AND EXTRAGALACTIC SOURCES

Our main approach to the interpretation of the data is to study color-color diagrams for the objects introduced in § 3 above; these diagrams are described and related to the physics of dust emission in § 4.1 below. In § 4.2, we address two poten-

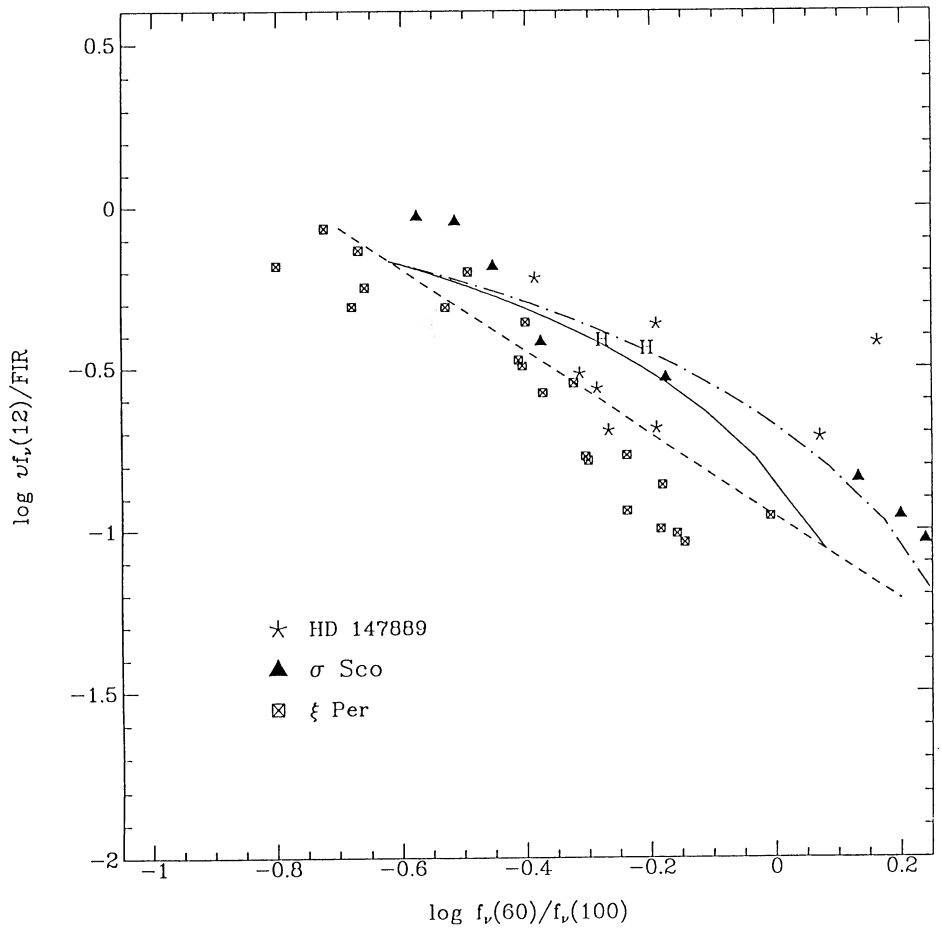

FIG. 1a

FIG. 1.—*IRAS* color-color diagram for emission from interstellar dust. The ordinate Γ represent a luminosity ratio between very small grains and larger classical grains; the abscissa Θ characterizes the interstellar radiation density in which the dust is observed. (*a*) Colors from the interstellar medium in the Milky Way, in the vicinity of three stars, as indicated by the different symbols; the data are from Ryter, Puget & Pérault (1987) and Boulanger et al. (1988) (see § 6 for more details). The colors move from the upper left-hand side toward the lower right-hand side of the diagram as the region sampled moves closer to the star. The adopted analytical fit to these data is drawn as the dashed line. The curved lines trace out the colors of combined emission from cirrus and active regions as an approximation to the integrated emission from galaxies (see § 5.3 and Appendix); the letter H marks the colors of a system whose luminosity is provided in equal parts by cirrus and active regions. (*b*) Integrated colors of the Virgo galaxies (§§ 3.1 and 4.1); the filled squares correspond to low uncertainty (<30%) on Γ, whereas the open squares correspond to data with higher uncertainty. (*c*) Colors of objects in the Bright Galaxy Sample (§ 3.2); the symbols correspond to the color ratio $f_\nu(25\ \mu m)/f_\nu(60\ \mu m)$, with circles used for values greater than 0.18, crosses for values between 0.12 and 0.18, and triangles for values smaller than 0.12. The broken line indicates the locus along which these data would have been distributed if the simplest selection effect (§ 4.2) had dominated the sample; the thick tracing through the distribution follows the median Γ in intervals of Θ, and the two thin lines are drawn, roughly parallel to the median, to encompass between them ~90% of the data points. (*d*) Colors of cold galaxies (§ 3.3) and of diffuse emission in the Milky Way. The filled and empty squares correspond to galaxies with, respectively, low and high (>30%) uncertainty on Γ. The letter S indicates the colors of the large-scale emission from the diffuse local interstellar medium (Boulanger & Pérault 1988); the letters C are for clouds within the Chamaeleon molecular complex; letters U and T are, respectively, for the integrated colors of the Ursa Major and Taurus molecular clouds.

tial biases that might affect the color-color diagrams of our galaxy samples as a result of selection effects or other systematics and find them to be of no concern. Several physical mechanisms can affect the integrated infrared colors of galaxies as compared to those of molecular clouds or diffuse nebulae; these are discussed in § 4.3 in view of separating them out before proceeding with the interpretation of the colors in terms of the relative abundance of small grains (§ 5).

4.1. *The Data*

Based on the conclusions of § 2 above, the ratio of 12 μm to far-infrared luminosity is a reasonable estimator of the relative importance of very small and large classical grains. We define

$$\Gamma = \frac{\nu f_\nu(12\ \mu m)}{\int_{40\ \mu m}^{120\ \mu m} f_\lambda\, d\lambda} \simeq \frac{2.5 \times 10^{-13} f_\nu(12\ \mu m)}{\mathrm{FIR}}, \quad (1)$$

where

$$\mathrm{FIR} = 3.25 \times 10^{-14} f_\nu(60\ \mu m) + 1.26 \times 10^{-14} f_\nu(100\ \mu m). \quad (2)$$

FIR is a far-infrared flux (in W m^{-2} for f_ν in Jy) whose ratio to the total far infrared emission (say between 1 and 1000 μm) depends only weakly on the temperature of dust emitting in thermal equilibrium in the temperature range of 20–60 K (Helou et al. 1988). Γ is a valid estimator of the relative effective absorption cross sections of the small and large grains in a given radiation field under the assumptions (1) that the 12 μm emission is predominantly produced by small grains, whose properties alone determine the spectrum of the emission, and (2) that FIR tracks the total flux emitted by the large grains, a good approximation for temperatures between 20 and 60 K. In order to relate Γ to a mass ratio, one needs either an estimate

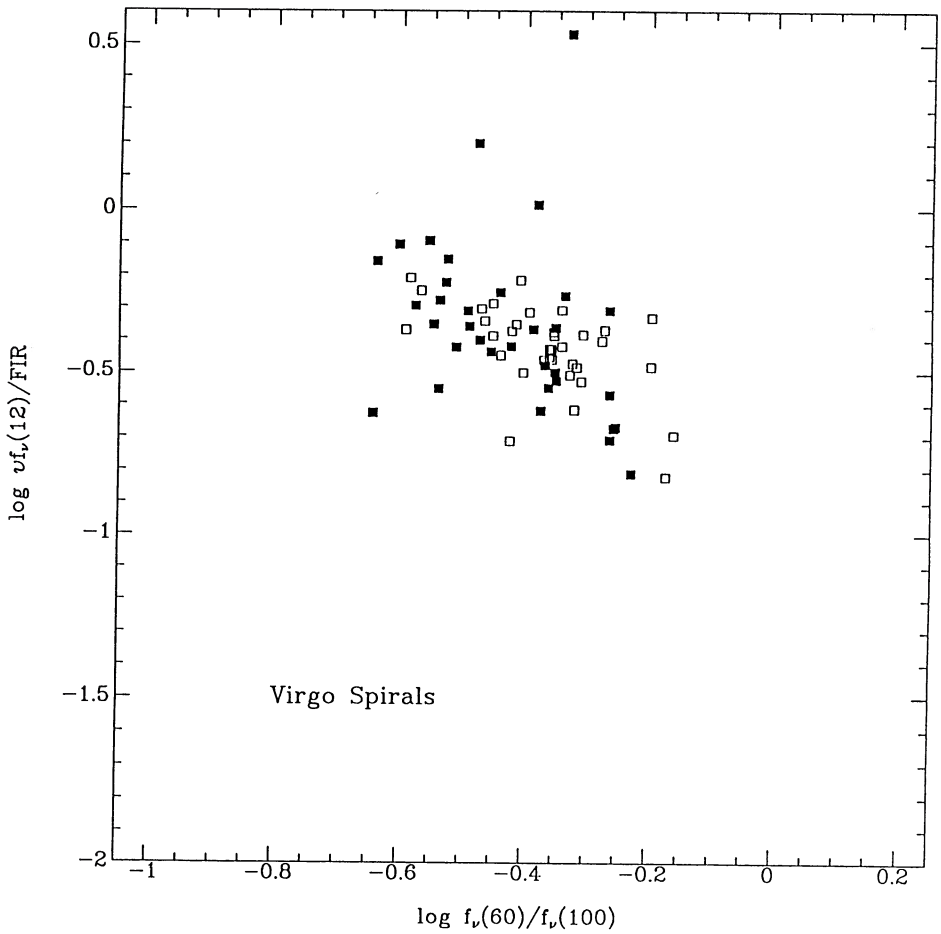

FIG. 1*b*

of the small grain emissivity at 12 μm in a given radiation environment, or a detailed model of both the intensity of the heating radiation and of the absorption efficiency of small grains in the ultraviolet to near-infrared range. Γ is unlikely to be simply proportional to the mass ratio of very small to classical grains and is difficult to interpret without an indication of the intensity of the radiation field responsible for heating the dust. Such an indication is provided by the ratio

$$\Theta = f_\nu(60\ \mu\text{m})/f_\nu(100\ \mu\text{m}) , \qquad (3)$$

which is to first order related to the temperature of large grains, and thereby to the intensity of the radiation field to which they are exposed.

We therefore present in Figure 1 a set of scatter diagrams of Γ vs. Θ, with Figure 1*a* showing data from the interstellar medium in the vicinity of three stars (Ryter, Puget, & Pérault 1987; Boulanger et al. 1988; see § 6 for more details). The broken line represents a rough fit to the data. Figure 1*b* shows the colors of the Virgo galaxies, with the objects whose Γ is uncertain by more than 30% appearing as open squares, and those with less uncertainty appearing as filled squares. Figure 1*c* contains data from the bright galaxy sample, with the different symbols now indicating different ranges in the $f_\nu(25\ \mu\text{m})/f_\nu(60\ \mu\text{m})$ color ratio, triangles for values smaller than 0.12, circles for values larger than 0.18, and crosses in between. Figure 1*d* shows data from the cold galaxy sample (the symbols reflect uncertainty as in Fig. 1*b*), as well as from nearby molecular clouds studied by Boulanger et al. (1990), and the diffuse local interstellar medium (the cosec$|b|$ law) from Boulanger & Pérault (1988).

The *IRAS* colors of galaxies have a distribution that follows, with considerable scatter, the general trend outlined by the local colors within nebulae. Could this agreement be induced by sample selection or analysis method?

4.2. *Selection Effects and Artifacts*

The defining condition for the *IRAS* bright galaxy sample (Fig. 2*c*) is the constraint $f_\nu(60\ \mu\text{m}) > 5.24$ Jy, so that most flux measurements at 60 μm would be expected to occur just above the limiting flux density; Figure 1 in Soifer *et al.* (1989) shows a broad peak in the distribution of $f_\nu(60\ \mu\text{m})$ centered near 8 Jy. In addition, the $f_\nu(12\ \mu\text{m})$ distribution displays a similar peak at 0.5 Jy. The simplest potential artifact would be for most points in the color-color diagram to lie near the locus defined by the combination of the two conditions: $f_\nu(60\ \mu\text{m}) = 8$ Jy and $f_\nu(12\ \mu\text{m}) = 0.5$ Jy. If $f_\nu(100\ \mu\text{m})$ is considered an independent variable, those two equalities define a curve in Figure 1 which satisfies the equation:

$$\Gamma = 1.25\Theta(2.58\Theta + 1)^{-1} , \qquad (4)$$

which is represented in Figure 1*c* by the broken line with a positive slope everywhere. This line is the trend likely to be

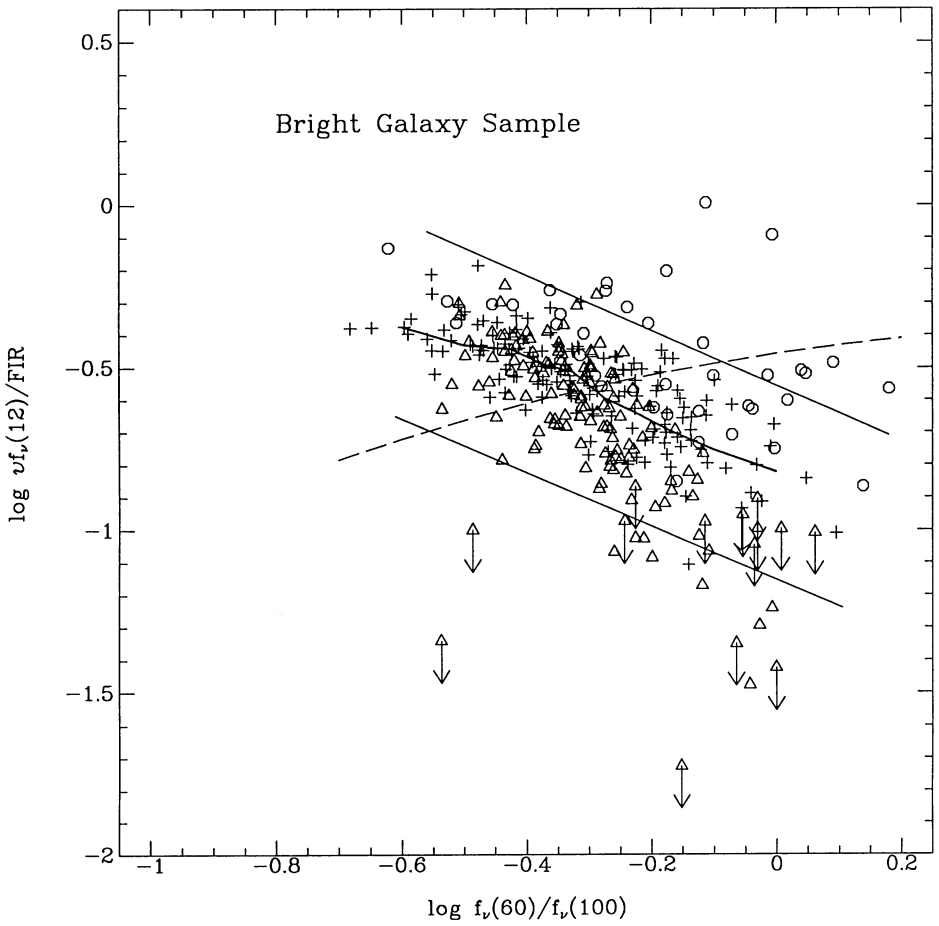

FIG. 1c

observed in the absence of real correlations among the colors of galaxies. Evidently, the distribution of points in Figure 1c does not follow this null trend, and reflects instead a nontrivial correlation between the colors.

Another potential bias may be introduced by plotting on Figure 1 two quantities which are not truly independent. Since $f_\nu(100\ \mu m)$ appears in the denominators of both Γ and Θ, one would expect the points in Figure 1 to be positively correlated, which is clearly not the case. On the other hand, $f_\nu(60\ \mu m)$ appears in the numerator of Θ and the denominator of Γ, and thus could potentially induce an "anticorrelation" between the two parameters. If such false dependence existed however, it would be characterized by a slope no steeper than roughly -0.5, which is flatter than the observed trend (slope $\simeq -1.3$) in Figure 1c.

Since the samples in Figures 1b and 1c behave similarly, although derived from orthogonal selection criteria, it is unlikely that other selection effects have affected the data severely. The distribution of data points in Figure 1 is therefore accepted as a reliable representation of the statistical behavior of the observables.

4.3. *Intrinsic Differences*

This section discusses three factors that affect the *IRAS* colors of galaxies but not those of nebulae, namely, the mixing of emission components, large optical depths, and heating of dust by active galactic nuclei rather than by stars only.

Figure 1 compares the colors of individual points within a nebula to the colors of an entire galaxy, representing superposition of many components with diverse colors. This integration should cause galaxies to appear slightly above the locus defined by the nebulae in Figure 1, thereby broadening the galaxy distribution. The solid line in Figure 1a illustrates this effect by showing the color track followed by a galaxy with a diffuse interstellar radiation density $u_C \simeq 0.5$ eV cm^{-3} (typical condition 100′ from ξ Per), in which an increasing fraction of the interstellar medium is embedded in a radiation density $u_W \simeq 30$ eV cm^{-3} (typical condition 5′ from ξ Per, and expected in starburst environments); the dotted line represents a similar track for $u_W \simeq 100$ eV cm^{-3}. The simple model used to generate these color tracks is presented in the Appendix. Even moderate amounts of material in the high-energy density environment tend to dominate the integrated emission of the galaxy, and one can see that the resulting colors are not very different from those of a medium submitted to a *uniform* high-radiation density. Furthermore, this result is relatively independent of the values used for u_C and u_W. It seems intuitively clear that a distribution of radiation densities is not able to alter more drastically the color-color diagram.

The infrared sources in very dusty galaxies may be embedded in dust which is optically thick at 12 μm and 25 μm, in which case they would tend to fall below the band defined by the other galaxies in Figure 1. For instance, the optical thickness of the 9.7 μm silicate feature in Arp 220 is $\tau(9.7\ \mu m) = 3$,

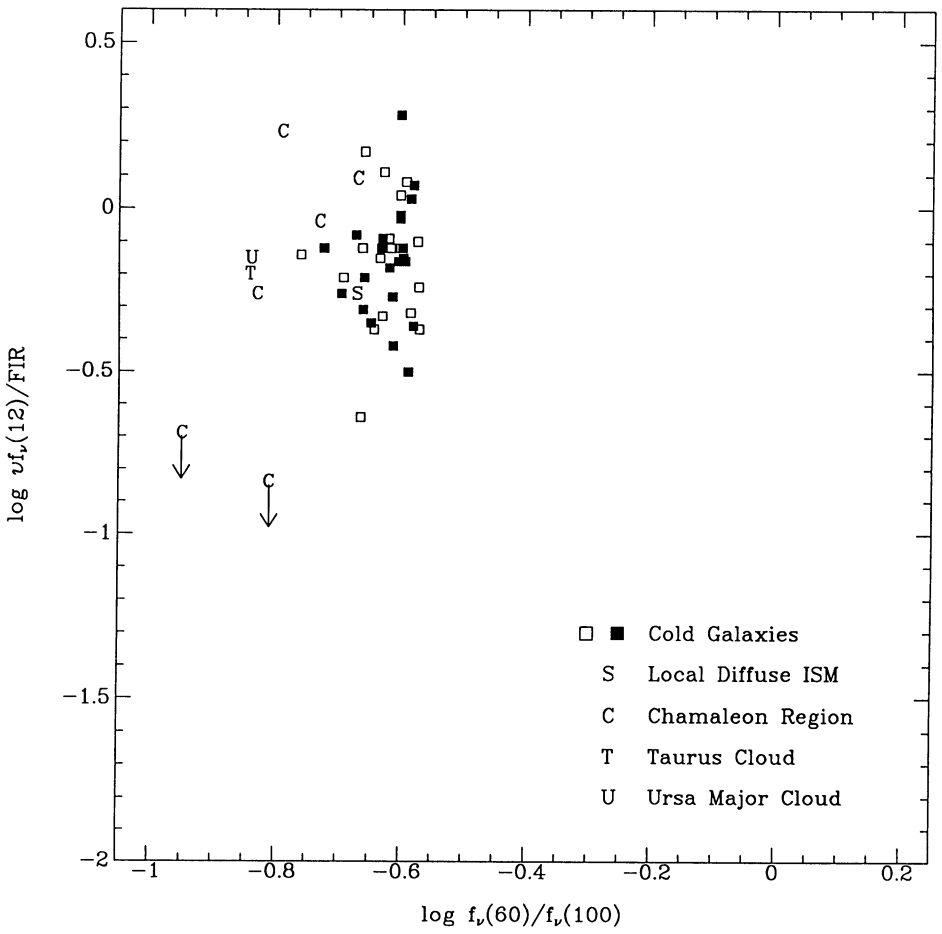

FIG. 1*d*

corresponding to an extinction $A_V = 50$ (Becklin & Wynn-Williams 1987), and an optical thickness averaged over the *IRAS* 12 μm band of ~ 1.6. One possible signature of very dusty objects is an exaggerated spectral slope in the mid-infrared due to differential optical depth of the embedding dust between 25 and 60 μm. Using Mezger, Mathis, & Panagia (1982), we estimate the average optical thickness over the *IRAS* bands and find that the emerging value of $f_\nu(25\ \mu\text{m})/f_\nu(60\ \mu\text{m})$ would be equal to the value at the source multiplied by $\exp[-0.56\tau(9.7\ \mu\text{m})]$. Although this treatment of the embedding dust is too simplistic (since the temperature of the emitting dust must vary with the optical depth at which it is located), steep spectral slopes in the mid-infrared can still be used to identify heavily embedded galaxy candidates. An additional diagnostic for such candidates is a large infrared-to-blue ratio, as discussed in § 5 below.

Infrared bright galaxies may host an active nucleus which introduces a nonthermal heating spectrum in the optical and the ultraviolet. (We adopt the conclusion reached by several recent studies, e.g., Sanders et al. 1989, that the infrared luminosity from radio-quiet quasars and active nuclei is dominated by thermal dust emission rather than a nonthermal component). This difference in the heating may lead to a far-infrared emission spectrum of the dust substantially different from that obtained when the dust is heated by stellar photospheres, primarily because of the wavelength dependence of the absorption cross sections of small and large grains. In addition, the harder heating spectrum probably depresses the abundance of very small grains, since they are known to be depleted in the vicinity of massive young stars (Ryter, Puget, & Pérault 1987; Boulanger et al. 1988). Seyfert galaxies have been associated with a relatively flat spectrum between 25 and 60 μm. A selection criterion of $f_\nu(25\ \mu\text{m})/f_\nu(60\ \mu\text{m}) > 0.35$ was proposed by de Grijp et al. (1985) to identify Seyfert activity. More recently, Wilson (1988) has found that $f_\nu(25\ \mu\text{m})/f_\nu(60\ \mu\text{m}) < 0.29$ is a reliable test for finding objects dominated by star formation, based on the morphology of active regions in galaxies. Here we adopt the more conservative condition $f_\nu(25\ \mu\text{m})/f_\nu(60\ \mu\text{m}) > 0.18$ to flag potential contamination by an active nucleus (as suggested for instance by Fig. 2 of Hill, Becklin, & Wynn-Williams 1988) and show all objects satisfying this condition as open circles in Figure 1*c*. Because there is no sharp separation between star-forming and Seyfert-like galaxies on this color ratio, our condition flags most Seyfert-like nuclei, but also some non-Seyferts. Interestingly, this condition turns out to be efficient at finding galaxies whose spectra do *not* reveal the near infrared aromatic features; it finds 21 of 24 such galaxies in the sample studied by Désert & Dennefeld (1988). Such galaxies are very likely to display evidence of Seyfert-like nuclear activity.

Thus galaxies with unusually steep or unusually shallow spectral slopes between 25 and 60 μm are likely to suffer from

extraneous effects, making them poorly suited to comparison with the properties of dust as observed in nearby nebulae.

5. COMPARISON RESULTS AND ABUNDANCE OF VERY SMALL GRAINS

Galaxies from both the Virgo sample (Fig. 1*b*) and the Bright Galaxy Sample (Fig. 1*c*) seem to follow the same distribution, reproducing the trend observed for the local colors within near-by nebulae (Fig. 1*a*), except that the bright galaxies spread out to larger values of Θ, corresponding to warmer color temperatures. The median Γ at each Θ for the bright galaxy sample (Fig. 1*c*) matches reasonably well the broken line in Figure 1*a* which corresponds to the model in the Appendix. Moreover, the dispersion in Γ at each Θ among galaxies is comparable to the dispersion in local colors within nebulae and increases clearly as Θ increases. The interval in log Γ holding half the galaxies is ~ 0.12 near log $\Theta = -0.5$, and grows to 0.3 or more around log $\Theta = 0$.

To understand the origin of the scatter in Γ, we have examined the galaxies with the largest deviations from the Galactic data or equivalently the median line. We traced in Figure 1*c* boundaries (shown as two thin lines) roughly parallel to the median line, and holding between them $\sim 90\%$ of all points; we then identified individually all objects outside of these boundaries. Thirteen out of 14 objects above the main body of the distribution have a ratio $f_\nu(25\ \mu\text{m})/f_\nu(60\ \mu\text{m}) > 0.18$ and may therefore be suspected of hosting an active nucleus (see § 4.3 above). The 15 objects falling below the lower boundary all turn out to be very active or peculiar galaxies with $f_\nu(25\ \mu\text{m})/f_\nu(60\ \mu\text{m}) < 0.12$. They are NGC 5728, NGC 5104, Arp 148 = VV 32, NGC 2623, UGC 5101, UGC 8387, UGC 6436, NGC 1266, CGCG 1510.8+0725, MCG +08-18-012, IRAS 17132+5313, IRAS 10565+2448, Arp 220 = IC 4553/4554, IC 860, IIIZw 035. These are good candidates for being optically thick at 12 μm (see § 4.3 above), as corroborated by their unusually high infrared to visible emission ratio, which ranges from about ~ 10 to over 100. The only exception is NGC 5728 which has a ratio of ~ 2. By contrast, the galaxies which belong to both the Virgo sample and the infrared-bright sample have infrared to visible luminosity ratios in the range of one-half to five. Thus if NGC 5728 is excluded from the statistics, Virgo galaxies on one hand and the objects with unusually small values of Γ on the other define two completely separate intervals on a scale of infrared-to-visible ratio.

Given that most of the dispersion in Γ at log $\Theta > -0.25$ is due to complications extraneous to the emission by very small grains in the normal interstellar medium, we are led to the conclusion that the relative abundance of very small grains (at constant heating) does not vary among galaxies by as much as the scatter in Γ would seem to indicate. Among quiescent objects in the Bright Galaxy Sample (Fig. 1*c*) with log Θ near -0.5, the population dispersion in Γ is only $\sim 25\%$. Because this number is based on very few objects, we decided to pursue the question of relative abundance of very small grains by examining cold galaxies, i.e., those with the lowest values of Θ. Such galaxies are well suited for this purpose because (1) most of their dust is probably at the same (cirrus-like) temperature, (2) their 12 μm emission is less likely to be contaminated by very hot dust in or near H II regions, and (3) they are less likely to be harboring active nuclei.

However, because these galaxies are quiescent, they are characterized by low surface brightness emission and are often resolved by the *IRAS* detectors at 12 μm. As a result, their fluxes are hard to estimate, and about half of them (20 out of the 43 mentioned in § 3.3) have Γ uncertain by 30% or more (1 σ). These 20 have $\langle \log \Gamma \rangle = -0.20$, with an rms dispersion on log Γ of ~ 0.19, which may be entirely due to the measurement uncertainties on $f_\nu(12\ \mu\text{m})$. The remaining 23 galaxies, with a typical uncertainty on log $f_\nu(12\ \mu\text{m})$ of 0.08, yield a somewhat lower dispersion on Γ, namely, 0.15 (log scale) or 40%, which may be considered an upper limit on the intrinsic dispersion of Γ among galaxies. The relative abundance of very small grains is therefore roughly constant among galaxies, with a rms dispersion of 40% or less.

6. DISCUSSION

Figure 1*a* is derived from detailed observations of the interstellar medium in the surrounding of three stars located in quite diverse environments. The star HD 147889 (spectral type B2) has not formed an H II region, except for a very compact and weak radio continuum source (Falgarone & Gilmore, 1981); it is heavily obscured and appears surrounded mostly by molecular gas. The star σ Sco (type B1 III) is surrounded by a partly ionized medium of lower density (Ryter, Puget, & Pérault 1987). The star ξ Per (type O7.5 III) is ionizing the extensive bright California nebula NGC 1499 (Boulanger et al. 1988). The infrared emission from dust in all three environments shows roughly the same behavior in a color-color diagram, with the general roll-off of Γ as a function of Θ revealing depressed emission by very small grains relative to large classical grains, due either to selective destruction or to reduced relative emissivity. In either case, it is reasonable to assume that the effect is linked to the enhanced radiation field close to the star. The highest excitation condition probed by the data in Figure 1*a* corresponds to $f_\nu(60\ \mu\text{m})/f_\nu(100\ \mu\text{m}) = 1.8$, or a radiation density of ~ 100 eV cm^{-3}.

The same relationship between *local* colors in the interstellar medium appears to be followed by the *global* colors of galaxies in Figure 1*b* and 1*c*. The main implication is that the typical normal galaxy (i.e., one which is not heavily dust-embedded or housing an active nucleus) has an interstellar dust population with properties very similar to those of the local interstellar medium in the Milky Way. As mentioned in § 4.3 above, the colors of normal galaxies are dominated by their most active regions. Thus the behavior observed around nearby stars is universal, in that the emission from small grains relative to large grains depends primarily on one parameter, the intensity of the heating radiation field, and that it is always depressed at high-energy densities.

At similar interstellar heating conditions (traced by the 60–100 μm color ratio), the relative abundance of very small and classical large grains is the same in the Milky Way as in other galaxies and is roughly constant among galaxies, with a rms population dispersion smaller than 40% and possibly as low as 25%. Furthermore, the relative emissivity of large and small grains is observed to depend on one parameter only, namely, the interstellar heating conditions. We conclude that the underlying relative abundance of small and large grains, i.e., at low radiation densities, is the same in the more luminous and active "normal" disk galaxies as in the quiescent ones; in other words, the quiescent sections of active galaxies must resemble in their colors the quiescent galaxies, and vice versa. We do not address here potential variations of the relative abundance in systems with different levels and histories of metal enrichment, such as elliptical, Magellanic irregular, or

blue compact dwarf galaxies (Sauvage, Thuan, & Vigroux 1990).

A significant implication of this analysis is that quiescent or very dense and cold molecular clouds cannot dominate the far-infrared emission from galaxies, given the disparity in the observed colors in Figure 1*d*; even in cold galaxies, the component most likely to dominate is the diffuse interstellar medium. In the more active normal spiral galaxies, more intensely heated dust clearly dominates the emission. Thus the conclusion we reach about the constancy of the small-to-large grain ratio in cold galaxies applies *a fortiori* to the diffuse interstellar medium of galaxies rather than to sites associated with ongoing star formation activity.

This constancy of small-to-large grain ratio in the diffuse medium contrasts somewhat with the situation in molecular cloud complexes, where large variations in the ratio are observed on scales ranging from a few tenths of a parsec to a few parsecs. To illustrate this point, data from Table 1 of Boulanger et al. (1990) on the integrated colors of molecular clouds (Taurus and Ursa Major) and of well-defined segments of clouds within the Chamaeleon complex have been plotted in Figure 1*d*. There is visibly more scatter in Γ in molecular clouds, which is interpreted by Boulanger et al. to reflect true variations in the abundance of very small grains rather than variations in the heating. It follows that the detailed processes (on the molecular cloud scale) whereby grains can be added to or removed from the interstellar medium are different for the small and the large grains. These local variations however must average out when the emission is integrated over a whole galaxy, resulting in a global relative abundance which is independent of a galaxy's morphological type, judging by the statistics of Γ in the cold galaxy sample. If small and large grains have independent sources and sinks, then a constant relative abundance implies that the steady state galaxy-wide abundance reached by each grain population must be constant from galaxy to galaxy; it follows that the source-to-sink ratio for each grain population is independent of galaxy morphology, and therefore of the stellar population, and the interstellar medium mass. A simpler interpretation is that small and large grains are created and destroyed in the same sites and processes, and thus their relative abundance is independent of the stellar population or other morphology-related parameters in a galaxy; in this case, the local variations of Γ in molecular clouds reflect the second-order effects such as temporary condensation of small particles onto larger grains, which is the interpretation favored for entirely different reasons by Boulanger *et al.* (1990).

The value of $\nu f_\nu(12\ \mu\text{m})/\text{FIR}$ in the case of quiescent galaxies with cold dust may be translated into a ratio (albeit an uncertain one) of carbon content in small and large grains. Puget & Léger (1989) suggest an estimate for the luminosity per carbon atom in PAHs and in very small grains irradiated by the local interstellar radiation field, based on the absorption properties of these populations. They also estimate, based on the reflection nebula spectrum by Sellgren et al. (1985), that the luminosity emitted by PAHs is given by $1.1\nu f_\nu(12\ \mu\text{m})$. The combination of these two estimates allows the $12\,\mu$m luminosity to be transformed into a carbon atom count. On the other hand, Draine & Anderson (1985) compute for the same radiation field an emissivity at 100 μm in the range of 0.8 to 1 MJy sr^{-1} per 10^{20} H cm^{-2}, which may be used to translate the 100 μm flux into a mass of hydrogen. The resulting translation formula agrees with the Hildebrand (1983) derivation, using a temperature obtained from $f_\nu(60\ \mu\text{m})/f_\nu(100\ \mu\text{m})$, and the calibration at 250 μm, if we assume for the cold dust $f_\nu(60\ \mu\text{m})/f_\nu(100\ \mu\text{m}) = 0.2$, and an emissivity proportional to ν. Given all this, the observed $\nu f_\nu(12\ \mu\text{m})/\text{FIR}$ value translates into $\sim 20\%$ of all carbon tied up in PAHs, in addition to $\sim 17\%$ tied up in very small grains (Puget & Léger 1989). However, Allamandola, Tielens, & Barker (1989) derive a fraction of carbon tied up in these species ~ 10 times smaller, based on essentially the same data, but different assumptions for the emissivity at 12 μm. More work is clearly needed to reduce the disparity between various estimates of the emissivity of very small grains.

7. SUMMARY

From the analysis of the *IRAS* colors of three samples of galaxies, optically bright Virgo spirals, infrared bright systems (selected at 60 μm), and galaxies cold in the far-infrared [selected for $f_\nu(60\ \mu\text{m})/f_\nu(100\ \mu\text{m}) < 0.25$], we find that

1. The global *IRAS* colors of galaxies follow well the colors of the interstellar medium in a variety of environments observed in the Milky Way. The ratio, Γ, of 12 μm flux to far-infrared flux depends on one parameter only, namely the color ratio between 60 and 100 μm, which relates to the intensity of the radiation field heating the dust.
2. Both the local and global color variations result from the response of the small (PAHs and particles up to 100 Å in size) and large grain populations to the variation in the energy density of the heating radiation. Γ is systematically depressed at higher energy densities, at least up to $u \sim 100$ eV cm^{-3}.
3. The relative abundance of very small and large grains, as measured by the ratio Γ at the same heating conditions, is rather constant among a wide variety of galaxies, with a dispersion smaller than 40%. This suggests that while the two populations are quite distinct in their behavior, they are closely coupled in terms of formation and destruction on the scale of galaxies.

In contrast to molecular clouds, where the small-to-large grain ratio is observed to vary more substantially, the size spectrum of interstellar dust grains seems to reach a universal equilibrium distribution in the diffuse media of normal galaxies, dictated only by the "mean" radiation field intensity in the galaxy.

We would like to thank our referee, J.-L. Puget, and R. J. Laureijs for helpful comments on the manuscript. C. R. is indebted to C. Beichman for hospitality, and to the Jet Propulsion Laboratory for financial support, during part of this work at IPAC in the summer of 1988. We would like to thank B. Rampante of the Istituto Calvino for an illuminating perspective on this topic, Mary Ellen Barba for help with the manuscript, and Linda Hermans for help with the figures. This research is supported through the IRAS Extended Mission Program by the Jet Propulsion Laboratory, California Institute of Technology, under a contract with the National Aeronautics and Space Administration.

APPENDIX

COLORS OF GALAXIES WITH QUIESCENT AND ACTIVE COMPONENTS

We consider a galaxy whose interstellar medium is exposed to a uniform interstellar radiation density u_C, expressed in eV cm^{-3} in what follows. A fraction of the interstellar material is submitted to a higher radiation density u_W, such that the emission spectra from the two phases (C and W) are combined with amplitudes p and $1 - p$, respectively. We derive the locus traced out in Figure 1 by the infrared colors of this galaxy as p varies from 0 to 1. We start by identifying an analytic fit to the data in Figure 1*a*:

$$\Gamma \equiv \nu f_\nu(12\ \mu\text{m})/\text{FIR} = 0.11\Theta^{-1.28} \tag{A1}$$

FIR is defined and Γ discussed in § 4.1 above. From Figure 3 of Ryter, Puget, & Pérault (1987), we deduce

$$\Theta \equiv f_\nu(60\ \mu\text{m})/f_\nu(100\ \mu\text{m}) \equiv 0.3u^{0.39} \tag{A2}$$

and from Figure 4 of Puget, Léger, & Boulanger (1985), we write the power radiated (in watts per H atom) by the warm dust:

$$\Phi \equiv \nu\phi_\nu(60\ \mu\text{m}) + \nu\phi_\nu(100\ \mu\text{m}) = 5.5 \times 10^{-30}u\ , \tag{A3}$$

$$\Phi = 1.21 \times 10^{-28}\Theta^{2.57}\ . \tag{A4}$$

From Helou et al. (1988), we obtain

$$\text{FIR}/\Phi = (0.42 + 1.08\Theta)/(1 + 1.67\Theta)\ . \tag{A5}$$

Let us define the quantities $f_{1,C}$, $f_{3,C}$ and $f_{4,C}$ to be, respectively, $f_\nu(12\ \mu\text{m})$, $f_\nu(60\ \mu\text{m})$, and $f_\nu(100\ \mu\text{m})$ emitted from the region exposed to the radiation field u_C and similarly $f_{1,W}$, $f_{3,W}$, and $f_{4,W}$ as the flux densities originating in a region with radiation density u_W. Given u_C and u_W, it is a simple matter to derive the colors from equations (A2) and (A3) as a function of p and combine them to produce the observables

$$\Theta = [pf_{3,W} + (1 - p)f_{3,C}]/[pf_{4,W} + (1 - p)f_{4,C}]\ , \tag{A6}$$

$$\Gamma = [p\nu f_{1,W} + (1 - p)\nu f_{1,C}]/[p\text{FIR}_C + (1 - p)\text{FIR}_W]\ , \tag{A7}$$

which now describe a quiescent disk (u_C) housing an active region defined by u_W and p.

The locus of Γ vs Θ traced out as p increases from 0 to 1 is represented in Figure 1*a* for a galaxy with $\Theta_C = 0.24$ (corresponding to $u_C \simeq 0.5$ eV cm^{-3}) housing an active region with $\Theta_W = 1.2$ (for $u_W \simeq 30$ eV cm^{-3}); a similar locus is shown for a galaxy with the same Θ_C, but with $\Theta_W = 2$ (for $u_W \simeq 100$ eV cm^{-3}).

REFERENCES

Allamandola, L. J. 1989, in IAU Symp. 135, Interstellar Dust, ed. L. J. Allamandola & A. G. G. M. Tielens (Dordrecht: Kluwer), p. 129
Allamandola, L., Tielens, A. G. G. M., & Barker, J. R. 1985, ApJ, 290, L25
———. 1989, ApJS, 71, 733
Andriesse, C. D. 1978, A&A, 66, 169
Becklin, E. E., & Wynn-Williams, C. G. 1987, in Star Formation in Galaxies, NASA CP 2466, ed. C. J. Lonsdale (Washington, DC: NASA)
Binggeli, B., Sandage, A., & Tammann, G. A. 1985, AJ, 90, 1681
Boulanger, F., Beichman, C., Désert, F. X., Helou, G., Pérault, M., & Ryter, C. 1988, ApJ, 332, 328
Boulanger, F., Falgarone, E., Puget, J.-L., & Helou, G. 1990, ApJ, 364, 136
Boulanger, F., & Pérault, M. 1988, ApJ, 330, 964
Cohen, M., Allamandola, L. J., Tielens, A. G. G. M., Bregman, J., Simpson, J. P., Witteborn, F. C., Wooden, D., & de Muizon, M. 1986, ApJ, 341, 246
Cox, P., Krugel, E., & Mezger, P.G. 1986, A&A, 155, 380
Cox, P., & Mezger, P. G. 1989, A&AR, 1, 49
de Grijp, M. H. K., Miley, G. K., Lub, J., & De Jong, T. 1985, Nature, 314, 240
Désert, F. X., & Dennefeld, M. 1988, A&A, 206, 227
Draine, B. T., & Anderson, N. 1985, ApJ, 292, 494
Draine, B. T., & Lee, H. M. 1984, ApJ, 285, 89
Duley, W. W. 1989, in IAU Symp. 135, Interstellar Dust, ed. L. J. Allamandola & A. G. G. M. Tielens (Dordrecht: Kluwer), p. 141
Falgarone, E., & Gilmore, W. 1987, A&A, 95, 32
Giard, M., Pajot, F., Caux, E., Lamarre, J. M., & Serra, G. 1989, A&A, 215, 92
Gillett, F. C., Forrest, W. J., & Merrill, K. M. 1973, ApJ, 183, 87
Gillett, F. C., Kleinmann, D. E., Wright, E. L., & Capps, R. W. 1975, ApJ, 198, L65
Ghosh, S. K., Drapatz, S., & Peppel, U. C. 1986, A&A, 167, 341
Helou, G. 1986, ApJ, 311, L33
Helou, G., Khan, I. R., Malek, L., & Boehmer, L. 1988, ApJS, 68, 151
Hildebrand, R. H. 1983, QJRAS, 24, 267
Hill, G. J., Becklin, E. E., & Wynn-Williams, C. G. 1988, ApJ, 330, 737.
IRAS Catalogs and Atlases: Point Source Catalog 1988, Joint *IRAS* Science Working Group (Washington, DC: NASA)
IRAS Science Team 1986, A&AS, 65, 607
Léger, A., & Puget, J.-L. 1984, A&A, 137, L5
Mathis, J. S., Rumpl, W., & Nordsieck, H. K. 1977, ApJ, 217, 425
Merrill, K. M., Soifer, B. T., & Russell, R. W. 1975, ApJ, 200, L37
Mezger, P., Mathis, J. S., & Panagia, N. 1982, A&A, 105, 372
Moshir, M., et al. 1989, Explanatory Supplement to the *IRAS* Faint Source Survey (Pasadena: JPL)
Pajot, F., Boissé, P., Gispert, R., Lamarre, J. M., Puget, J. L., & Serra, G. 1986, A&A, 157, 393
Phillips, M. M., Aitken, D. K., & Roche, P. F. 1984, MNRAS, 207, 35
Price, A. J. 1981, AJ, 86, 193
Puget, J.-L., & Léger, A. 1989, ARAA, 27, 161
Puget, J.-L., Léger, A., & Boulanger, F. 1985, A&A, 142, L19
Rice, W., Boulanger, F., Viallefond, F., Freedman, W., & Soifer, B. T. 1990, ApJ, in press
Russell, R. W., Soifer, B. T., & Willner, S. P. 1977, ApJ, 217, L149
Ryter, C., Puget, J. L., & Pérault, M. 1987, A&A, 186, 312
Sanders, D. B., et al. 1989, A&A, 213, L5
Sauvage, M., Thuan, T. X., & Vigroux, L. 1991, A&A, submitted
Schwering, P. B. W. 1988, Ph.D. thesis, University of Leiden
Sellgren, K. 1984, ApJ, 277, 623
Sellgren, K., Werner, M. W., & Dinerstein, H. L. 1983, ApJ, 277, 623
Soifer, B. T., Sanders, D. B., Madore, B. F., Neugebauer, G., Danielson, G. E., Elias, J. H., Lonsdale, C. J., & Rice, W. L. 1987, ApJ, 320, 238
Soifer, B. T., Boehmer, L., Neugebauer, G., & Sanders, D. B. 1989, AJ, 98, 766
Walterbos, R. A. M., & Schwering, P. B. W. 1987, A&A, 180, 27
Weiland, J. L., Blitz, L., Dwek, E., Hauser, M. G., Magnani, L., & Rickard, L. J. 1986, ApJ, 306, L101
Willner, S. P., Soifer, B. T., Russell, R. W., Joyce, R. R., & Gillett, F. C. 1977, ApJ, 217, L121
Wilson, A. S. 1988, A&A, 206, 41
Young, J. S., Kleinmann, S. G., & Allen, L. E. 1988, ApJ, 334, L63